

**$(^3\text{He}, t)$  reaction mechanism via the  $^{38}\text{Ar}(^3\text{He}, t)^{38}\text{K}$  reaction at 40 MeV**G. Bruge,\* M. S. Zisman, A. D. Bacher,<sup>†</sup> and R. Schaeffer\**Lawrence Berkeley Laboratory, University of California, Berkeley, California 94720*C. J. Zeippen<sup>†</sup> and J. M. Loiseaux*I. S. N. Grenoble, Grenoble, France*

(Received 17 April 1978)

The  $^{38}\text{Ar}(^3\text{He}, t)^{38}\text{K}$  reaction has been studied using a 40 MeV  $^3\text{He}$  beam. Angular distributions for 26 levels are presented and theoretical analysis of the results has been carried out. Firstly, the conclusions of a macroscopic study of the  $^{38}\text{K}$  level spectrum are presented. Secondly, the difficulties encountered using a one-step microscopic model to describe the five lowest states of  $^{38}\text{K}$  are discussed. Thirdly, the improvements obtained by including two-step contributions in our microscopic model are shown and the importance of the transitions occurring via the  $[(^3\text{He}, \alpha) + (\alpha, t)]$  channel is emphasized.

NUCLEAR REACTIONS  $^{38}\text{Ar}(^3\text{He}, t)$ ,  $E=40$  MeV; measured  $\sigma(\theta)$ ; resolution 75 keV. Microscopic DWBA analysis; coupled-channel analysis; deduced  $L$  transfers; deduced strengths of microscopic  $(^3\text{He}, t)$  effective force.

## I. INTRODUCTION

The present work is concerned with the "charge-exchange" reaction  $^{38}\text{Ar}(^3\text{He}, t)^{38}\text{K}$  at 40 MeV. In recent years, increasing use has been made of the  $(^3\text{He}, t)$  reaction as a spectroscopic tool.<sup>1</sup> In fact, it is a very powerful method of reaching nuclei which could otherwise be obtained only through transfer reactions. The charge-exchange reaction is generally described in terms of a microscopic model. In this framework, the  $(^3\text{He}, t)$  reaction is very similar to a reaction involving inelastic scattering of a light projectile. However, in the case of  $(^3\text{He}, t)$  charge exchange, the cross sections are very small, and multistep processes can be a very important part of the reaction mechanism.<sup>2,3</sup>

Great progress has been made in our knowledge concerning the  $(^3\text{He}, t)$  reaction mechanism. Usually, an effective force interacting between the projectile center of mass and the excited nucleon in the target is used.<sup>4</sup> It seems that enough information has been gathered in the case of nuclei with simple structures to enable one to make a reasonable choice of the force parameters and to start a spectroscopic study of more complex nuclei.<sup>1,4-10</sup>

It has been established that a tensor component is required in the nucleon-nucleon force if one wants to explain the angular distributions of unnatural-parity levels.<sup>6,7</sup> In fact it seems that there are two distinct types of  $(^3\text{He}, t)$  transitions which should show different sensitivity to the tensor term.<sup>7</sup> We have a great amount of information concerning the first type of transition and a very small amount concerning the second type. One of the reasons for studying the  $^{38}\text{Ar}(^3\text{He}, t)^{38}\text{K}$  reaction is a desire to clarify our ideas about the

apparent difference between the two types of transitions. To this end we have compared the parameter values for the effective nucleon-nucleon force in an  $(f_{7/2} \rightarrow f_{7/2})$  transition (type 1) for the reaction  $^{48}\text{Ca}(^3\text{He}, t)^{48}\text{Sc}$  to those in a  $(d_{3/2} \rightarrow d_{3/2})$  transition (type 2) for the reaction  $^{38}\text{Ar}(^3\text{He}, t)^{38}\text{K}$ , using various final states. Then, we increased the complexity of the wave functions representing the  $^{38}\text{Ar}$  and  $^{38}\text{K}$  nuclei, and also that of the transition operator by including two-step processes. We have concentrated our efforts on the first five levels of  $^{38}\text{K}$ , since they are well separated in our experiment and their spins and parities are quite well known.

The first part of our theoretical analysis deals with the choice of optical parameters and with the assignment of transferred  $L$  values to the  $^{38}\text{K}$  levels populated through the  $(^3\text{He}, t)$  reaction. Where possible comparison is made with other results.<sup>11,12</sup> Besides the usual one-step microscopic description of the  $(^3\text{He}, t)$  reaction mechanism, it has also been possible to evaluate the importance of two-step transitions because of the existence of new codes allowing for coupled-channel calculations (in particular Ref. 13).

## II. EXPERIMENTAL PROCEDURE

The experiment was performed using a 40 MeV  $^3\text{He}$  beam from the Berkeley 88-inch cyclotron. The target was argon gas (enriched to 94.4%  $^{38}\text{Ar}$ ) at a pressure of 120 Torr which was contained in a cell having a thin (0.68 mg/cm<sup>2</sup>) nickel entrance foil and a 2.1 mg/cm<sup>2</sup> Havar exit foil. Tritons were detected by telescopes consisting of 0.25 mm  $\Delta E$  and 3 mm  $E$  detectors which fed a Goulding-Landis particle identifier.<sup>14</sup> The ex-

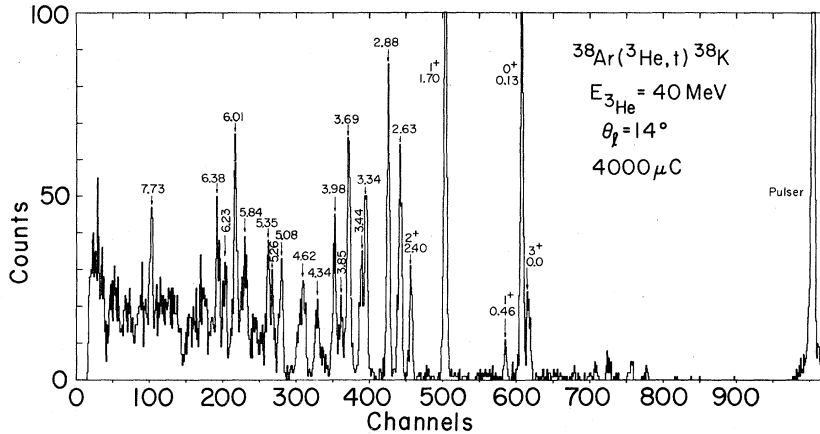


FIG. 1. Triton energy spectrum from the  $^{38}\text{Ar}(^3\text{He}, t)^{38}\text{K}$  reaction at  $\theta_l = 14^\circ$ .

perimental spectrum is displayed in Fig. 1; the overall energy resolution is 75 keV full width at half maximum (FWHM). Triton groups corresponding to 26 states in  $^{38}\text{K}$  up to an excitation energy of about 8 MeV have been observed; angular distributions have been measured from  $\theta_{\text{c.m.}} = 11^\circ$  to  $50^\circ$ .

### III. MACROSCOPIC ANALYSIS OF THE RESULTS

The unstable  $^{38}\text{K}$  nucleus has been investigated through both decay experiments and direct pick-up reactions. Most of the results have been reviewed by Endt and Van der Leun.<sup>11</sup> Apart from a few low-lying states, the  $^{38}\text{K}$  level structure appears to be rather complicated. The spins and parities of the first five states [i.e., ground state ( $3^+$ ), 0.13 MeV ( $0^+$ ,  $T=1$ ), 0.46 MeV ( $1^+$ ), 1.70 MeV ( $1^+$ ), and 2.41 MeV ( $2^+$ ,  $T=1$ )] are quite well established, but since those of the higher-lying states are rather ambiguous, one has to take the features of every experiment into account in order to derive proper information about them.

Taking advantage of the fact that they are well understood, we shall use extensively the lowest five levels as reference states in the next sections to discuss the various possible mechanisms for the  $^{38}\text{Ar}(^3\text{He}, t)^{38}\text{K}$  reaction. For the sake of simplicity, we shall consider first the macroscopic model in order to discuss the relationship between the assigned  $L$  values and the spins and parities of the first five states of  $^{38}\text{K}$ . The analysis will then be extended to the higher-lying states.

#### A. The first five levels of $^{38}\text{K}$ and the choice of the optical parameters

We have tested extensively the influence of optical parameters on the angular distributions. Although any reasonable parameter choices give typical diffractive shapes which allow one to de-

termine unambiguously the dominant  $L$  transfer, the quality of the obtained fit obviously depends, to a certain extent, on the particular set chosen. The following procedure has thus been adopted:

(a) Many optical potentials were tested and the angular distribution for the  $0^+$  IAS (isobaric analog state of the  $^{38}\text{Ar}$  ground state), at 0.13 MeV in  $^{38}\text{K}$ , was used as a probe of their adequacy.

(b) For the other states, the transferred  $L$  values were extracted from experiment. As we had a double aim, i.e., to get a good basis for the attribution of  $L$  values to the higher-lying states, but also to test more elaborate reaction mechanisms for the lowest states, special care was taken to dispose of most of the ambiguities which could be due to the optical parameters.

In the case of the lowest five states, whose total angular momenta  $J$  are known, the usual selection rules for one-step processes were tested:

$$(-)^{\Delta L} = \pi \begin{cases} \Delta L = J \text{ for natural-parity states,} \\ \Delta L = J \pm 1 \text{ for unnatural-parity states.} \end{cases}$$

All the calculations were performed using the macroscopic formalism included in the code DWUCK.<sup>15</sup> The same optical parameters were taken for both the incoming channel and the form factor. Qualitatively, four sets of parameters, taken, respectively, from Refs. 5, 16, 17, and 18, give a good fit for the  $0^+$  state (see Fig. 2). The angular distributions for the other states ( $1^+$  to  $3^+$ ) are displayed in Fig. 3, which shows the fits obtained with the first and the last potential sets only. The calculated cross sections have been arbitrarily normalized to the maximum of the experimental angular distribution.

One can see the following:

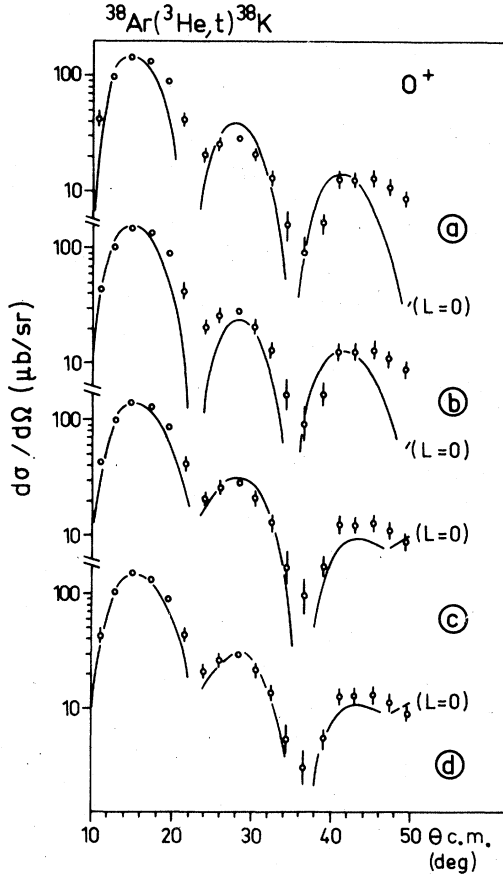


FIG. 2. Choice of the best optical potential parameters using the experimental 0.13 MeV ( $0^+$ ,  $T=1$ ) IAS of  $^{38}\text{K}$  as a probe of their adequacy. (a) Ref. 5, (b) Ref. 16, (c) Refs. 17, 18, (d) Refs. 17, 18 with  $r_{0c} = 1.25$  fm.

(a) Satisfactory agreement is obtained for the  $3^+$  ground state with an  $L=4$  angular distribution. The second maximum is essentially in phase with an  $L=2$  curve, but no  $L=4+L=2$  mixture gave a good overall fit; the amount of  $L=2$  which is necessary to fit the second maximum completely spoils the agreement at forward angles.

(b) No agreement can be obtained for the 0.458 MeV  $1_1^+$  state if we restrict ourselves to the  $L=0$  or  $L=2$  patterns allowed in a one-step transition. On the contrary, a reasonable fit is given only by an  $L=1$  calculated curve, in contradiction with the parity selection rule. One must note that this case is different from the previous one in that no agreement at all can be obtained even for a portion of the experimental angular distribution with the expected  $L=2$  or  $L=0$  curves. We were unable to find an optical potential set which could solve this problem without spoiling the agreement for the other states (in particular for the other  $1^+$  state). This is reminiscent of the  $L=1$  shape found for

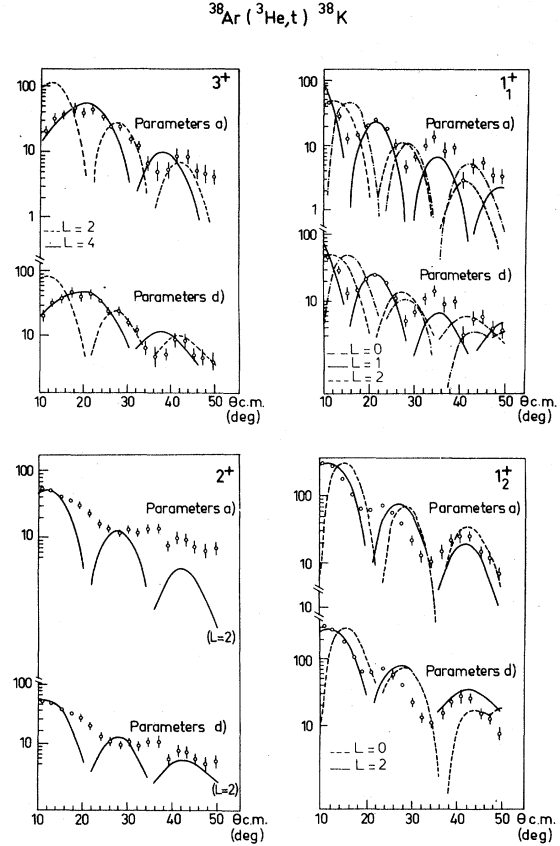


FIG. 3. Macroscopic calculations for the g.s. ( $3^+$ ), 0.458 MeV ( $1_1^+$ ), 1.704 MeV ( $1_2^+$ ) and 2.405 MeV ( $2^+$ ) states of  $^{38}\text{K}$ , using two of the optical potential sets selected from Fig. 2. (See Table I.)

some  $0^+ \rightarrow 0^+$  transitions observed in the  $(^3\text{He}, t)$  reaction,<sup>19</sup> and may be considered as a signature of the presence of second-order effects, in particular the  $[(^3\text{He}, \alpha) + (\alpha, t)]$  process.<sup>2,3,20</sup>

(c) In contrast with the previous case, good agreement is obtained for the  $1_2^+$  state at 1.704 MeV with a calculated  $L=2$  angular distribution, as is usual for such a  $(^3\text{He}, t)$  transition.<sup>5</sup> Summing  $L=2$  and  $L=0$  calculated curves does not particularly improve the fit because only a very weak  $L=0$  contribution is allowed by the experimental data. One should notice that the measured angular distribution for this state is out of phase with the data for the 0.458 MeV  $1_1^+$  state (see Fig. 3).

(d) Only the slope is properly reproduced for the  $2^+$  level at 2.405 MeV which does not have a diffractive structure, although the calculated angular distribution predicts one. This lack of structure for the  $2^+$  state is not explained in this model. The nature of the optical potentials we chose can be questioned but we have obtained good

fits using them for other nuclei ( $^{48}\text{Sc}$  and  $^{52}\text{Mn}$ ).<sup>4,5</sup> We believe that this particular shape of the  $2^+$  angular distribution can be attributed to the presence of second-order contributions, although we would not consider this to be as clear evidence for their existence as is the change in shape of the 0.458 MeV  $1^+$  angular distribution.

As we have not found a potential set which could give very good agreement for all five experimental distributions, we adopt the set of parameters which provides the best overall agreement. One can see, looking at Figs. 2 and 3, that the differences between the displayed fits are unimportant, except perhaps in the case of the  $2^+$  level, for which the slope is slightly better if one uses potential set (d) instead of set (a). Nevertheless, it is fair to say that a great number of optical

parameter sets are essentially equivalent as far as our macroscopic analysis is concerned. Potentials including spin-orbit terms have been used and the nonlocality corrections available in the code DWUCK<sup>15</sup> have been tested. They do not markedly affect the final results. Thus, we shall concentrate below on the two parameter sets given in Table I.

### B. Higher-lying levels of $^{38}\text{K}$

Although the present paper is concerned primarily with the first five levels of  $^{38}\text{K}$ , our data for the higher-lying states provide potentially useful information. For this reason the experimental angular distributions for these higher-lying states are displayed in Figs. 4(a) and 4(b). One can see that most of them show significant

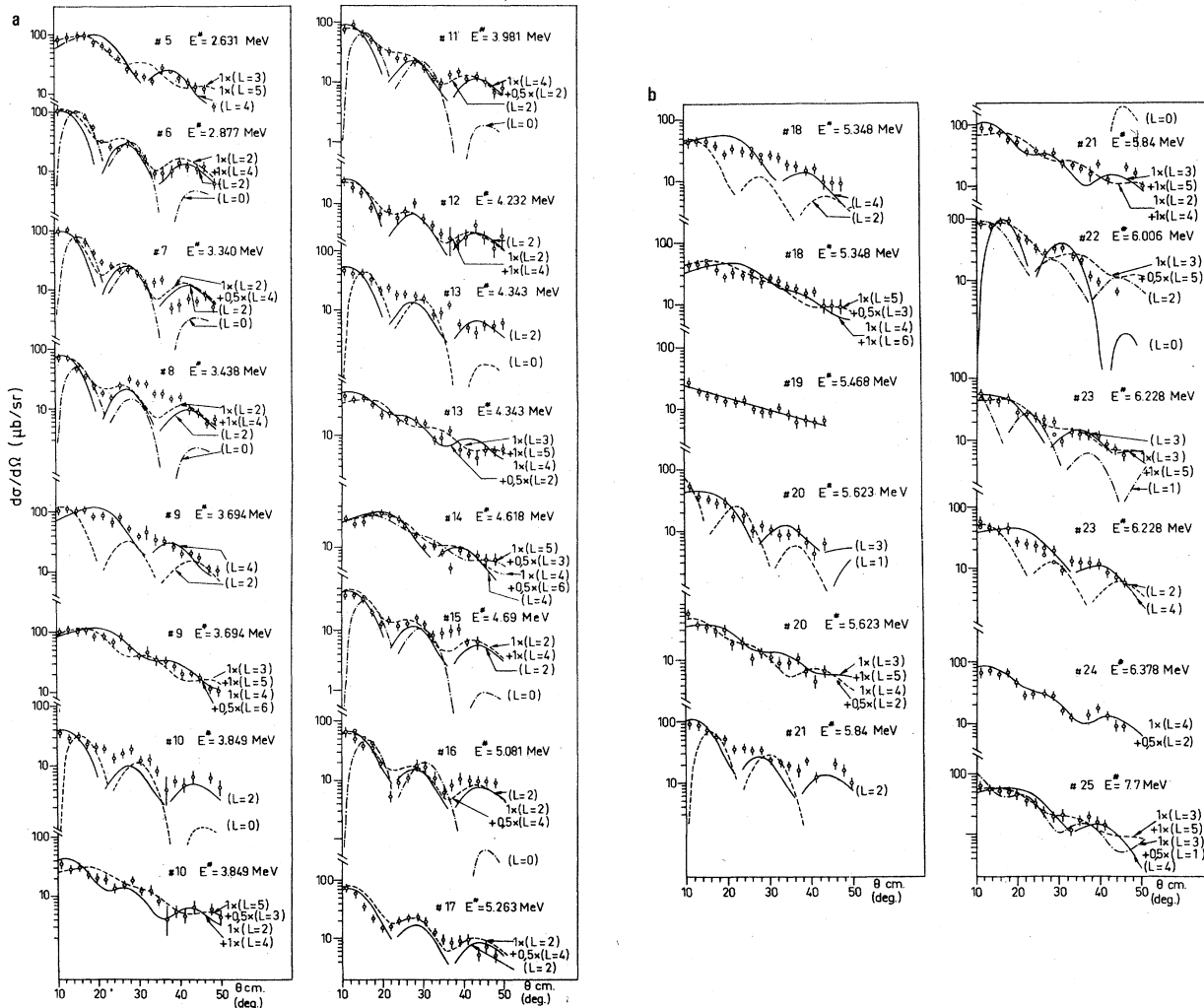


FIG. 4. (a) and (b) Experimental and calculated angular distributions for the higher-lying states of  $^{38}\text{K}$  using macroscopic calculations only. To obtain copies of the experimental data, see Ref. 34.

TABLE I.  $^3\text{He}$  and Triton optical potentials used in the present calculations.

| Particle        | Set | $V$<br>(MeV) | $r_v$<br>(fm) | $a_v$<br>(fm) | $W$<br>(MeV) | $r_w$<br>(fm) | $a_w$<br>(fm) | $W_s$<br>(MeV) | $r_{ws}$<br>(fm) | $a_{ws}$<br>(fm) |
|-----------------|-----|--------------|---------------|---------------|--------------|---------------|---------------|----------------|------------------|------------------|
| $^3\text{He}^a$ | (a) | 150.7        | 1.22          | 0.7           | 23.5         | 1.5           | 0.8           | -0.96          | 1.5              | 0.8              |
| $t^a$           |     | 143.7        | 1.22          | 0.7           | 23.5         | 1.5           | 0.8           | 0.96           | 1.5              | 0.8              |
| $^3\text{He}^b$ | (d) | 175.2        | 1.145         | 0.784         | 13.96        | 1.587         | 0.633         |                |                  |                  |
| $t^c$           |     | 152          | 1.24          | 0.684         | 19.6         | 1.48          | 0.771         |                |                  |                  |

<sup>a</sup> Reference 5.<sup>b</sup> Reference 17.<sup>c</sup> Reference 18.

diffraction shapes. Unfortunately, because of the 75 keV experimental resolution, many of the observed triton groups may correspond to multiplets. Clearly the level density for  $^{38}\text{K}$  is rather high above 5 MeV excitation.

The curves in Fig. 4 are theoretical angular distributions computed with DWUCK and arbitrarily normalized to the data. The calculations employed the optical parameter set (d) from Table I. The quality of fit and the conclusions we reached would not be altered if set (a) of Table I were chosen.

Our first aim in the comparison of theory to experiment was to propose probable transferred  $L$  values. Due to the energy resolution problems mentioned above, we cannot claim to make firm  $L$  assignments but only to provide indications which may be useful for subsequent investigations. In order not to overlook any possibilities, we have considered all plausible  $L$ 's and  $L$  mixtures. We believe our data rule out  $L$  values which are not included in Fig. 4. Our results show that in most cases a single  $L$  value is dominant, implying three possible values for  $J^\pi$ . For those levels with significant diffraction shapes, our "dominant"  $L$  values are mainly  $L = 2$ . However, considering the experimental problems and the possibility of  $L$  mixtures, it should be emphasized that we do not suggest that all of the high-lying  $^{38}\text{K}$  states have even  $L$  values.

Our results can be compared to other information on  $^{38}\text{K}$  such as the compilation of Endt and Van der Leun.<sup>11</sup> In particular we can compare with the results of Fenton *et al.*,<sup>12</sup> who studied  $^{38}\text{K}$  in the same excitation energy range via the  $^{39}\text{K}(^3\text{He}, \alpha)$  reaction. Despite our poorer energy resolution, the  $(^3\text{He}, t)$  reaction is clearly less selective than the  $(^3\text{He}, \alpha)$  reaction, populating many more states in  $^{38}\text{K}$ . However, in terms of proposed level schemes in the two reactions, there are no major discrepancies. In view of the present situation, more data would clearly be useful in order to properly understand the high-lying level scheme of  $^{38}\text{K}$ .

#### IV. MICROSCOPIC MODEL

We shall consider first one-step transitions only, in order to compare transitions in the  $sd$  shell observed here with transitions in the  $f_{7/2}$  shell, which are quite well known.<sup>7</sup> The angular distributions obtained this way obey the parity selection rule  $(-)^{\Delta L} = \pi$ , and only even  $L$  transfers are allowed. Our macroscopic analysis has already shown this rule is not valid for some transitions. Second-order effects, namely the contributions via the  $[(^3\text{He}, \alpha) + (\alpha, t)]$  channel will then be included, in order to see whether a better description can be obtained in this way. In this section, we shall again restrict ourselves to the five lowest levels whose structure is fairly well known.<sup>21-23</sup>

##### A. First-order transitions

The DWBA amplitude we use for the  $(^3\text{He}, t)$  reaction has been described in detail in Ref. 7. The transition occurs via an effective projectile-target nucleon interaction

$$V(r) = V_\tau f(r) + V_{\sigma\tau} f(r) \vec{\sigma}_1 \cdot \vec{\sigma}_2 + V_{T\tau} g(r) S_{12} \quad (1)$$

using the notation of Ref. 7.

Our main purpose in this section will be to determine whether the interaction strengths  $V_\tau$ ,  $V_{\sigma\tau}$ ,  $V_{T\tau}$  needed to reproduce the magnitudes of the  $^{38}\text{Ar}(^3\text{He}, t)^{38}\text{K}$  reaction cross sections are consistent with those obtained for a large selection of other nuclei. It was found previously that the effective interaction needed to describe the  $(^3\text{He}, t)$  reaction as a one-step process was fairly independent of the particular shell-model level the particles were in.<sup>7</sup> On the other hand, there was a strong  $L$  dependence ( $L =$  angular momentum transfer) which can be explained<sup>2,3,20</sup> by the existence of second-order contributions via the  $[(^3\text{He}, \alpha) + (\alpha, t)]$  process. However, all the transitions considered were of the type  $j = l + \frac{1}{2} \rightarrow j' = l' + \frac{1}{2}$  (type 1). The results of Ref. 7 suggested that the properties of the one-step  $j = l - \frac{1}{2} \rightarrow j' = l' - \frac{1}{2}$  transitions (type 2) were drastically different.

The tensor force is very strong for unnatural-parity transitions and dominates for type 1 transitions.<sup>6,7</sup> On the other hand, the tensor force is very weak for type 2 transitions. In other words, using the same values for  $V_{\sigma\tau}$  and  $V_{T\tau}$  for both type 1 and type 2 transitions results in vastly different cross section magnitudes in an  $(f_{7/2} \rightarrow f_{7/2})^{3+}$  and a  $(d_{3/2} \rightarrow d_{3/2})^{3+}$  transition, if one considers a single-step mechanism only. A severe test for the adequacy of the one-step description is therefore to check whether both  $(d_{3/2} \rightarrow d_{3/2})$  transitions, and  $(f_{7/2} \rightarrow f_{7/2})$  transitions, as seen for instance in the  $^{42}\text{Ca}(^3\text{He}, t)^{42}\text{Sc}$  and  $^{48}\text{Ca}(^3\text{He}, t)^{48}\text{Sc}$  reactions,<sup>5,7,24</sup> can be reproduced by an interaction such as that in Eq. (1) using the same parameters (essentially  $V_\tau$  for natural-parity transitions and  $V_{T\tau}$  for unnatural-parity transitions). Unfortunately, the only type 2 transitions studied experimentally,<sup>25</sup>  $p_{1/2} \rightarrow p_{1/2}$  in  $^{14}\text{C}(^3\text{He}, t)^{14}\text{N}$  and  $^{14}\text{N}(^3\text{He}, t)^{14}\text{O}$ , indicated that neither a pure central<sup>25</sup> nor a central + tensor<sup>26</sup> force could reproduce the shape of the observed angular distributions. Whether the fault lies with the optical model treatment or with an inadequate description of the transition operator is not clear. However, the measurements do suggest<sup>26</sup> that the central force required for type 2 unnatural-parity transitions is about four times stronger than the upper limit determined<sup>7</sup> from type 1 transitions. It was therefore particularly interesting to study the  $^{38}\text{Ar}(^3\text{He}, t)^{38}\text{K}$  reaction to try and clarify the situation.

For type 1 transitions, the previously obtained strengths were<sup>7</sup>

$$V_\tau \sim 6 \text{ to } 7 \text{ MeV for } L = 0,$$

$$V_{T\tau} \sim 3 \text{ MeV}.$$

The parameter  $V_{\sigma\tau}$  is not well determined, but there is definitely an upper limit<sup>4,7</sup> to its strength since a dominant  $\vec{\sigma}_1 \cdot \vec{\sigma}_2$  term would lead to an incorrect angular distribution,<sup>4,6,7</sup>

$$V_{\sigma\tau} \sim 0 \text{ to } 5 \text{ MeV}.$$

In Ref. 7,  $V_{\sigma\tau}$  has been arbitrarily taken equal to  $V_{T\tau}$ . In the analysis we report here the results have also been found to be insensitive to the precise choice of  $V_{\sigma\tau}$ , and we shall not comment further on the determination of that parameter.

Various descriptions have been proposed for the  $0^+ - 3^+$  multiplet. According to the wave functions of Dieperink and Glaudemans,<sup>21</sup> or those of Wildenthal *et al.*<sup>22</sup> which reproduce the observed  $\beta$  transition rates rather well, three of the five  $^{38}\text{K}$  levels below 2.4 MeV [ $3^+$  (g.s.),  $0^+$  (0.13 MeV), and  $2^+$  (2.41 MeV)] are mainly built from the  $(d_{3/2}^{-2})$  configuration, while the other two levels [ $1_1^+$  (0.46 MeV) and  $1_2^+$  (1.70 MeV)] are composed of  $(d_{3/2}^{-2})$ ,

$(d_{3/2}^{-1}s_{1/2}^{-1})$ , and other components. Although Dieperink and Glaudemans,<sup>21</sup> and Wildenthal *et al.*<sup>22</sup> restrict themselves to configurations composed of two holes in the  $sd$  shell, Skouras<sup>23</sup> allows for two particle-four hole admixtures but considers the  $T = 1$  ( $0^+$  and  $2^+$ ) states only.

Because the natural-parity transitions depend only on the strength of  $V_\tau$ , and the unnatural-parity transitions on the strength of  $V_{T\tau}$ , the values of these parameters are very simply obtained by adjusting the magnitudes of the calculated cross sections to the experimental ones. The results are given in Table II, where a comparison is made with the values obtained for the  $f_{7/2}$  transitions in mass 48. The 0.458 MeV ( $1_1^+$ ) state has not been included, since a one-step process forces the calculated angular distribution to be either an  $L = 0$  or  $L = 2$  shape, excluding  $L = 1$ .

Several general features can be noticed. First, the strength required for the  $0^+$  and  $2^+$  states is consistent with the one observed (Table II) for the  $^{48}\text{Ca}(^3\text{He}, t)^{48}\text{Sc}$  reaction.<sup>24</sup> The calculations of Ref. 7 have been redone, using more recent data<sup>24</sup> than those available at the time<sup>5</sup>; they are fairly insensitive to configuration mixing. In the case of the  $1^+$  and  $3^+$  states, if one assumes a pure  $(d_{3/2}^{-2})$  wave function, the strength needed for the tensor force is much larger (a factor of 3) than the one required for the  $f_{7/2}$  transition. This is a huge discrepancy, as the cross sections would be 10 times too small for the  $^{38}\text{K}$  states if one used the same strengths as in the case of  $^{48}\text{Sc}$ . Configuration mixing, as provided by the wave functions of Dieperink and Glaudemans,<sup>21</sup> leads to a real improvement for the  $1^+$  state, but does not help to rectify the discrepancy for the  $3^+$  state. One might wonder whether the absence of (2p-4h) admixtures in the wave functions might be responsible for the remaining gap. Indeed, a transition from the  $[(f_{7/2}^{-2})^{0+} - 4h]$  configuration in the  $^{38}\text{Ar}$  ground state to the  $[(f_{7/2}^{-2})^{3+} - 4h]$  configuration in the  $^{38}\text{K}$   $3^+$  state would be rather strong, despite its small weight in the wave function, since the matrix element of the tensor force  $S_{12}$  is much stronger for the  $f_{7/2}$  than for the  $d_{3/2}$  transition.<sup>7</sup> A rough estimate of these (2p-4h) admixtures for the  $T = 1$  states can be obtained from the wave functions of Skouras.<sup>23</sup> In that case, the (2p-4h) component represented about 16% of the wave function. Assuming the proportion of (2p-4h) is the same in the case of the  $1^+$  and  $3^+$  states, and choosing the sign of the amplitude to correspond to the most favorable case, one can bring the strength of  $V_{T\tau}$  needed for the  $^{38}\text{K}$   $3^+$  state down to a slightly smaller value (Table II) which is still, however, too large by nearly a factor of 3. (The corresponding angular distribution is shown in

TABLE II. Interaction strengths needed for the various calculations described in the caption to Fig. 6. The numbers in parentheses correspond to an approximate estimate of the 2p-4h admixtures in the wave functions (label S+A in Fig. 6).

| Level                 | $(d_{3/2} \rightarrow d_{3/2})$ | Dieperink and Glaudemans          | Skouras | $(f_{7/2} \rightarrow f_{7/2})^a$ |
|-----------------------|---------------------------------|-----------------------------------|---------|-----------------------------------|
| $0^+$                 | 6                               | 6                                 | 6       | 6.5 } $V_\tau$ (MeV)              |
| $2^+$                 | 9.5                             | 7.5                               | 9       |                                   |
| $1^+$                 | 11.5                            | 4.5                               | (4.5)   | 3.5 } $V_{T\tau}$ (MeV)           |
| $3^+$                 | 16.5                            | 25                                | (14)    |                                   |
| $\mu_\tau = 1.415$ fm |                                 | $\mu_{T\tau} = 0.878$ fm (DWBA74) |         |                                   |
|                       |                                 | $\mu_{T\tau} = 1.415$ fm (CHUCK)  |         |                                   |

<sup>a</sup> Taken from the  $^{48}\text{Ca}(^3\text{He}, t)$  reaction (see text).

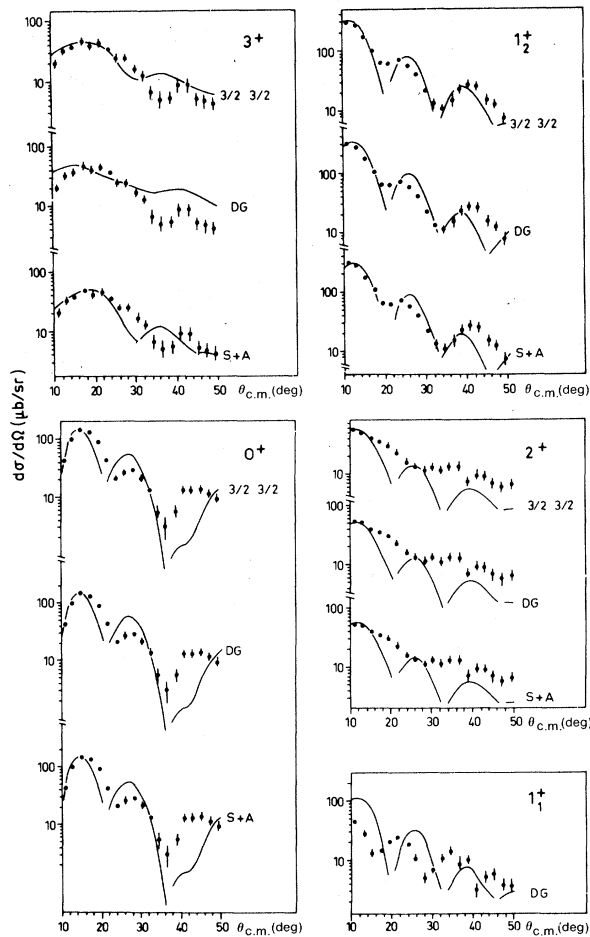


FIG. 5. Microscopic calculations for the lowest five levels of  $^{38}\text{K}$ . The curves labeled (3/2 3/2) correspond to pure  $(d_{3/2}^{-2})$  wave functions, those labeled DG to the  $sd$ -shell wave functions of Dieperink and Glaudemans<sup>21</sup>; those labeled S+A to the approximate estimate of the 2p-4h admixtures in the Skouras<sup>23</sup> wave functions. The microscopic interaction used is discussed in the text.

Fig. 5.) In addition, the actual magnitude of the (2p-4h) admixtures which contribute to the  $(^3\text{He}, t)$  transition is much smaller<sup>27</sup> than the one we have assumed here; in fact, it is probably negligible.

The  $0^+ - 1^+$  transition which displays an  $L = 1$  pattern cannot be reproduced by any microscopic calculation. This reminds one of the  $0^+ - 0^+$  transitions which have an  $L = 1$  shape.<sup>3, 19, 20</sup> The similarity between the two cases is remarkable. The  $L = 1$  shape of the  $0^+ - 0^+$  transitions was interpreted<sup>3</sup> as a manifestation of the nearly complete cancellation of the one-step process (due to configuration mixing) which allowed second-order contributions to show up. Indeed, in the case we are concerned with, configuration mixing leads to a destructive interference between the various components of the 0.458 MeV ( $1_1^+$ ) level, whereas the 1.7 MeV ( $1_2^+$ ) level displays a constructive interference.

The calculations were carried out using both codes DWBA74 (Ref. 28) and CHUCK.<sup>13</sup> The parameter values were the same, with the exception of  $\mu_{T\tau}$ . Indeed, to take into account the difference between the definition of the tensor force in the two codes, one must use two different values for the tensor force range. The results and conclusions were essentially the same in both cases. See Fig. 5 for the microscopic one-step angular distribution calculations.

In summary, the natural-parity transitions are very similar to those already observed, whereas the unnatural-parity, antianalog states raise two problems: the strength of the  $3^+$  level and the anomalous shape of the 0.458 MeV ( $1_1^+$ ) level. Both discrepancies seem to fall beyond the scope of the DWBA, and an investigation of possible second-order contributions is necessary.

#### B. Second-order effects

The transitions occurring via the  $[(^3\text{He}, \alpha) + (\alpha, t)]$  channel can be included in a way which

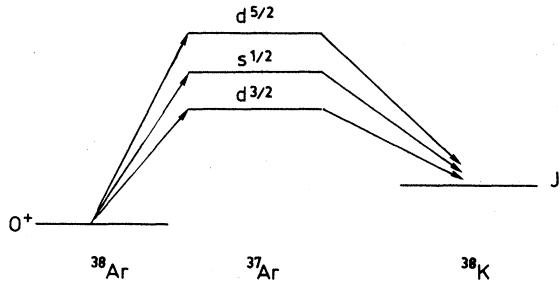


FIG. 6. Coupling scheme for the second-order transitions via the pickup channels. The  $^{37}\text{Ar}$  states are "model states" in the sense that they are obtained by removing a particle in the true  $^{38}\text{Ar}$  ground state without disturbing the other nucleons.

is now rather well known.<sup>20, 29, 30</sup> We have not solved the whole set of coupled equations, but we have taken into account only the contributions up to second order (Fig. 6). The intermediate states were assumed to be obtained by simply picking up a particle from the  $^{38}\text{Ar}$  ground state without disturbing the others. The spectroscopic amplitude for the  $(^3\text{He}, \alpha)$  process,  $S_n = \langle ^{37}\text{Ar} | a_n | ^{38}\text{Ar} \rangle$ , is then unity, since  $| ^{37}\text{Ar} \rangle = a_n | ^{38}\text{Ar} \rangle$  except for small corrections. Also, the spectroscopic amplitude for the  $(\alpha, t)$  process,

$$S_p = \langle ^{38}\text{K} | a_p^\dagger | ^{37}\text{Ar} \rangle = \langle ^{38}\text{K} | a_p^\dagger a_n | ^{38}\text{Ar} \rangle,$$

is then proportional to the same configuration mixing amplitudes as those which enter into the direct, one-step transition.

All the calculations of the present part of our study were done using the coupled-channels code CHUCK.<sup>13</sup>

#### 1. Choice of parameters

If one considers the magnitude of the second-order transition for each of the levels studied, one realizes that it is rather sensitive (the variation can be a factor of 2, in some cases) to the choice of optical parameters. Obviously the pa-

rameter set which gave us the best overall agreement with the experimental angular distributions of the five lowest levels of  $^{38}\text{K}$  in a one-step calculation is not necessarily the best choice if second-order effects are included. To illustrate this point with an example, we can consider the following alternatives: If we want to get reasonable two-step transition magnitudes using set (a) of Table I, we have to use the optical parameters suggested by Toyama<sup>20</sup> (or similar ones) for the  $\alpha$  particle, with a one-particle transfer strength  $D_0 = 480 \text{ MeV fm}^{3/2}$ . If we use set (d) in Table I, we should choose the  $V_R = 397.3 \text{ MeV}$  or  $V_R = 266.4 \text{ MeV}$  sets suggested by Weisser *et al.*<sup>31</sup> for the  $\alpha$  particle, with a  $D_0$  which is smaller than  $400 \text{ MeV fm}^{3/2}$  and even less for smaller values of  $V_R$ . (This behavior is very unfortunate. We have had problems in finding optical parameters consistent with the known value of  $D_0$  since large cross sections are usually obtained. The explanation for this behavior can probably be found in Ref. 32, which appeared after our work was completed.) As it is commonly accepted that the optical model  $V_R$  should be close to  $200 \text{ MeV}$  for  $\alpha$  particles and as the parameter  $D_0 \approx 480 \text{ MeV fm}^{3/2}$  is fairly well known, we shall restrict ourselves to the parameters listed in Table III. One should note that our  $^3\text{He}$  and triton optical parameter sets are very similar to the ones used by Toyama<sup>2</sup> and indeed they give comparable results; we prefer to keep our own parameters in order to assure consistency with the previous sections of our work. One remembers that the only real advantage, however small, of using set (d) of Table I instead of set (a) concerned the slope of the calculated curve for the  $2^+$  level of  $^{38}\text{K}$ . It will be shown shortly, however, that the introduction of second-order transitions in our calculations removes this difficulty. Therefore, we feel justified in our choice of parameters for the second-order transitions (see Table III).

TABLE III. Parameters used in the present calculation which allow for two-step processes (see text).

| Set     | Particle           | $V$                    | $r_v$ | $a_v$ | $W$            | $r_w$ | $a_w$ | $V_{s0}$ | $r_{s0}$ | $a_{s0}$ |
|---------|--------------------|------------------------|-------|-------|----------------|-------|-------|----------|----------|----------|
| $B+T$   | $^3\text{He}, t^a$ | [see Table I, set (a)] |       |       |                |       |       |          |          |          |
|         | $\alpha^{b,c}$     | 198.6                  | 1.458 | 0.502 | 19.8           | 1.51  | 0.79  |          |          |          |
|         | $\alpha^{b,d}$     | 183.7                  | 1.4   | 0.56  | 26             | 1.48  | 0.56  |          |          |          |
| Boulder | $^3\text{He}^e$    | 149.0                  | 1.2   | 0.72  | 32.2           | 1.4   | 0.88  | 10       | 1.2      | 0.72     |
|         | $t^e$              | 159.2                  | 1.2   | 0.72  | $41.5 - 0.32E$ | 1.4   | 0.84  | 10       | 1.2      | 0.72     |
|         | $\alpha^e$         | 200                    | 1.4   | 0.57  | $55.2 - 0.6E$  | 1.4   | 0.57  |          |          |          |

<sup>a</sup> Reference 5.

<sup>b</sup> Reference 2.

<sup>c</sup>  $A = 38$ .

<sup>d</sup>  $A = 48$ .

<sup>e</sup> Reference 31.



2.  $^{38}\text{Ar}(^3\text{He}, t)^{38}\text{K}$ 

Whatever optical parameters are chosen, the second-order transition dominates the  $3^+$  state when the tensor strength is adjusted to fit the  $^{48}\text{Ca} \rightarrow ^{48}\text{Sc}$   $3^+$  transition. Using the parameters of Table III, the second-order contribution has about the right magnitude for the  $3^+$  state of  $^{38}\text{K}$ . This gives us a prediction for the two-step process which shall no longer be modified. Figure 7 shows the theoretical results for the direct, two-step and combined processes, as well as experimental measurements for each of the five lowest

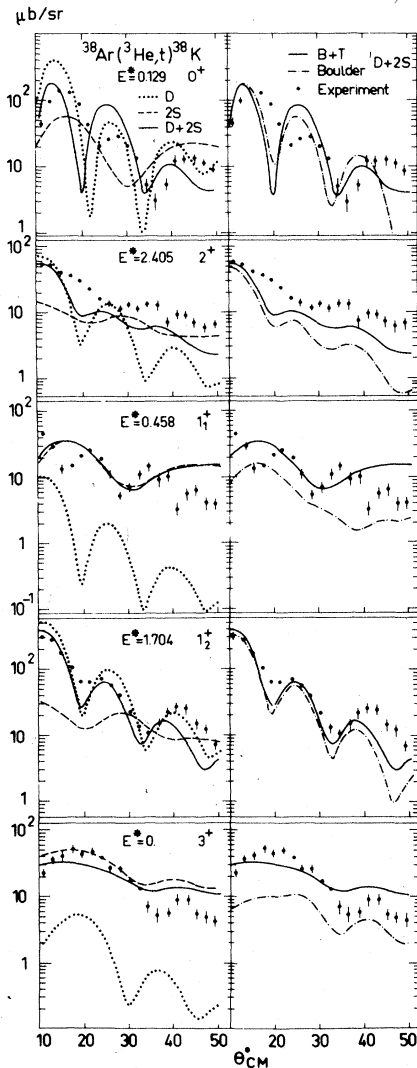


FIG. 7. Microscopic calculations ( $V_T = 12.5$  MeV,  $V_{Tr} = 7$  MeV) for the lowest five levels of  $^{38}\text{K}$ , allowing for two-step transitions. Curves for the direct, two-step and combined processes are shown. The microscopic interaction used is described in the text. The optical parameters are given in Table III.

levels of  $^{38}\text{K}$ . One can see that, in the case of the  $0^+$  and  $2^+$  levels, the second-order contribution alone is a factor of 2 too small at forward angles, but has the correct magnitude at angles beyond  $30^\circ$ , where the calculations involving a direct mechanism fit poorly. Also, if a central force  $V_T = 12.5$  MeV is used for both levels, one-step contributions provide just the missing strength at forward angles, and the interference between the two amplitudes leads to angular distributions in which both forward- and backward-angle experimental patterns are qualitatively reproduced. Thus, in the case of natural-parity states, it is possible to describe both levels using exactly the same parameters. In particular, one should notice that the lack of structure and the slope of the  $2^+$  level are well reproduced. [The theoretical results which are shown in the case of the  $2^+$  level have been obtained by using the wave functions of Dieperink and Glaudemans<sup>21</sup>; this leads to a better agreement than that obtained by simply assuming a  $(d_{3/2}^{-2})$  configuration.] As far as the unnatural-parity states are concerned, the two-step contribution alone explains the observed strength of both the 0.458 MeV  $1_1^+$  and  $3^+$  ground state, which could not be reproduced by a one-step calculation; on the other hand the second-order effect is too small by an order of magnitude for the 1.704 MeV ( $1_2^+$ ) state. Once again, we shall not discuss the value of the parameter  $V_{OT}$ ; that term of the force contributes only weakly to our transitions. If one uses a tensor force  $V_{Tr} = 7$  MeV for the  $3^+$  and both  $1^+$  levels, all these unnatural-parity states can be reproduced quite well. In this case also, it is possible to describe all the levels by using the same parameters. It should nevertheless be acknowledged that while the magnitude of the 0.458 MeV ( $1_1^+$ ) level is quite satisfactory and the shape is qualitatively reproduced, the precise form remains a problem. In brief, it seems we are fully justified to conclude that two-step processes including an intermediate  $\alpha$  particle are essential to explain the experimental results concerning the  $^{38}\text{Ar}(^3\text{He}, t)^{38}\text{K}$  reaction at 40 MeV. However, a more elaborate treatment of the second-order process still seems necessary.<sup>32,33</sup>

3.  $^{48}\text{Ca}(^3\text{He}, t)^{48}\text{Sc}$ 

As the specific choice of the different parameters has been shown to be crucial, we felt it was important to test the various values we used for  $A = 38$  in the case of  $A = 48$ . Figure 8 shows the theoretical curves for direct, two-step and combined transitions, together with experimental data. We show results for all  $(f_{7/2} \rightarrow f_{7/2})^{0^+ \rightarrow 7^+}$  transitions in the  $^{48}\text{Ca}(^3\text{He}, t)^{48}\text{Sc}$  reaction. Toyama<sup>2</sup> discussed this reaction previously, but

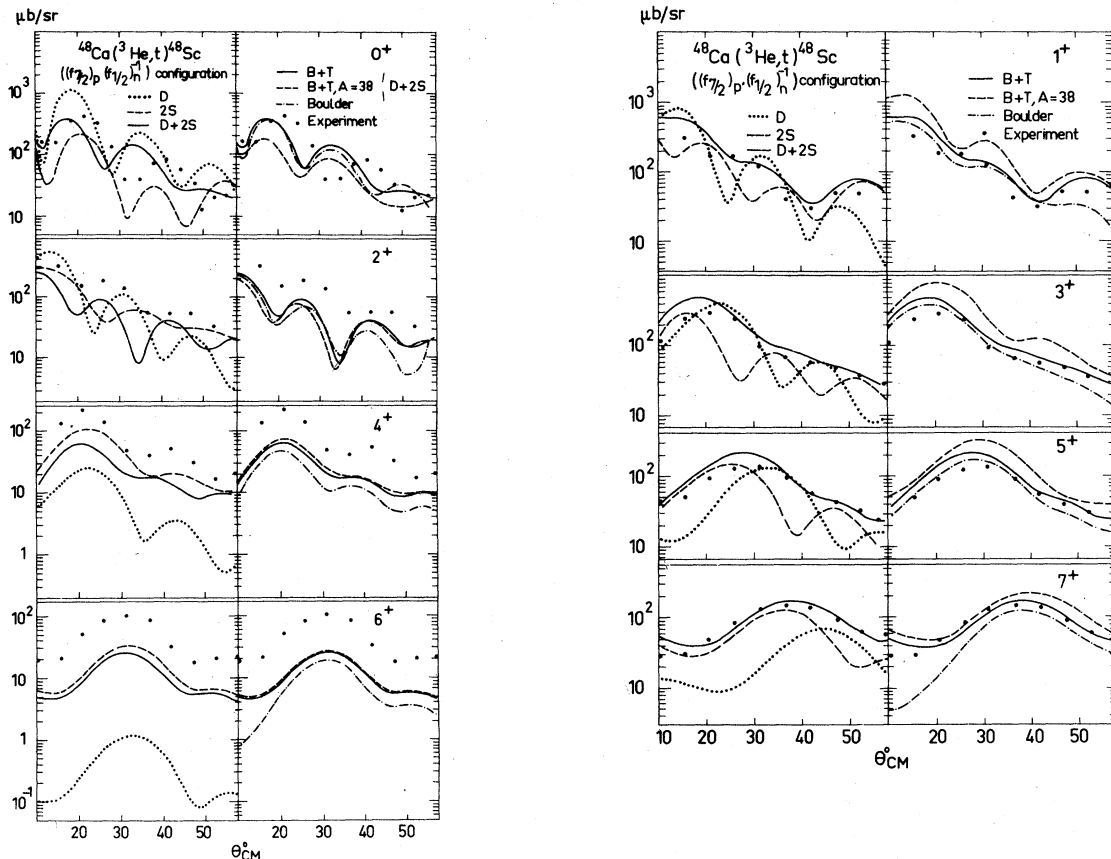


FIG. 8. Microscopic calculations ( $V_\tau = 15$  MeV,  $V_{T\tau} = 5$  MeV) for the  $f_{7/2}$  multiplet  $0^+ \rightarrow 7^+$  of  $^{48}\text{Sc}$ , allowing for two-step transitions: (a) natural parity states, (b) unnatural parity states. Curves for the direct, two-step and combined processes are shown, together with experimental data taken from Ref. 24. The microscopic interaction used is described in the text. The optical parameters are given in Table III.

restricted himself to natural-parity levels and to separate two-step and direct transitions. In our case, the strengths we have used to describe the  $(^3\text{He}, t)$  mechanism for  $A = 38$  are consistent with the requirements for  $A = 48$ . The theoretical cross sections are in satisfactory agreement with the experimental ones and the shapes of the theoretical curves are quite good. Our results are correct within a factor of 2: The natural-parity transitions are somewhat too weak, whereas the unnatural-parity transitions are slightly too strong. If we made the choice  $V_\tau \sim 15$  MeV and  $V_{T\tau} \sim 5$  MeV,

TABLE IV. Strength parameters for the one-step effective interaction contributing to the  $(^3\text{He}, t)$  reaction.

| Configuration                 | $V_\tau$<br>(MeV) | $V_{T\tau}$<br>(MeV) |
|-------------------------------|-------------------|----------------------|
| $d_{3/2} \rightarrow d_{3/2}$ | 12.5              | 7                    |
| $f_{7/2} \rightarrow f_{7/2}$ | 15                | 5                    |

we would reproduce the exact strength of the transitions to these 8 levels. We consider that a justification of the choice we made for the different parameters has been provided and that the apparent discrepancy between the two types of  $(^3\text{He}, t)$  transitions<sup>7</sup> has been greatly reduced. In Table IV the final values of  $V_\tau$  and  $V_{T\tau}$  are given. They are now nearly unique for all spins and targets.

## V. CONCLUSION

In the first part of our study, we have been able, using a macroscopic model, to help clarify the interpretation of the dense level spectrum of  $^{38}\text{K}$ . In the second part of the present paper convincing evidence has been given for the importance of a "combined" process in the explanation of  $(^3\text{He}, t)$  transitions. Indeed, it is necessary to include both a direct charge-exchange reaction and the transitions via an intermediate  $\alpha$  particle in the calculations in order to obtain a satisfactory description of the mechanism of the  $(^3\text{He}, t)$  reaction.

## ACKNOWLEDGMENTS

One of us (CJZ) wishes to express his hearty thanks to the French Government for financial support and to the ISN (Grenoble) and the CEN

(Saclay) for the competent attention, sympathy, and computing facilities, provided to him through-out his "Doctorat de troisième cycle" work. This work was done with support from the Division of Nuclear Science, Nuclear Physics Division, U. S. Department of Energy.

- \*Present address: CEN Saclay, B. P. No. 2, Gif-sur-Yvette, France.
- †Present address: Physics Department, Indiana University, Bloomington, Indiana 47401.
- ‡Present address: Observatoire de Paris, Section d'Astrophysique, 92190 Meudon, France.
- <sup>1</sup>In particular, see Argonne National Laboratory Informal Report No. PHY-1970A, January 1970 (unpublished), and references contained therein.
- <sup>2</sup>M. Toyama, Phys. Lett. **38B**, 147 (1972).
- <sup>3</sup>G. Bertsch and R. Schaeffer, Phys. Lett. **38B**, 159 (1972).
- <sup>4</sup>P. Kossanyi-Demay, P. Roussel, H. Faraggi, and R. Schaeffer, Nucl. Phys. **A148**, 181 (1970).
- <sup>5</sup>G. Bruge, A. Bussière, H. Faraggi, P. Kossanyi-Demay, J. M. Loiseaux, P. Roussel, and L. Valentin, Nucl. Phys. **A129**, 417 (1969).
- <sup>6</sup>E. Rost and P. D. Kunz, Phys. Lett. **30B**, 231 (1969).
- <sup>7</sup>R. Schaeffer, Nucl. Phys. **A164**, 145 (1971).
- <sup>8</sup>R. Sherr, T. S. Bhatia, D. Cline, and J. J. Schwartz, Ann. Phys. (N.Y.) **66**, 548 (1971).
- <sup>9</sup>J. R. Comfort, J. P. Schiffer, A. Richter, and M. M. Stautberg, Phys. Rev. Lett. **26**, 1338 (1971).
- <sup>10</sup>J. M. Loiseaux, G. Bruge, P. Kossanyi-Demay, Ha Duc Long, A. Chaumeaux, Y. Terrien, and R. Schaeffer, Phys. Rev. C **4**, 1219 (1971).
- <sup>11</sup>P. M. Endt and C. Van der Leun, Nucl. Phys. **A214**, 403 (1973).
- <sup>12</sup>J. A. Fenton, T. H. Kruse, N. Williams, M. E. Williams, R. N. Boyd, and W. Savin, Nucl. Phys. **A187**, 123 (1972).
- <sup>13</sup>P. D. Kunz and E. Rost, Program CHUCK, Univ. of Colorado, Boulder, Colorado (unpublished).
- <sup>14</sup>F. S. Goulding, D. A. Landis, J. Cerny, and R. H. Pehl, Nucl. Instrum. Methods **31**, 1 (1964).
- <sup>15</sup>P. D. Kunz, Program DWUCK, Univ. of Colorado, Boulder, Colorado (unpublished).
- <sup>16</sup>J. W. Leutzelschwab and J. C. Hafele, Phys. Rev. **180**, 1023 (1969).
- <sup>17</sup>E. F. Gibson, B. W. Ridley, J. J. Kraushaar, M. E. Rickey, and R. H. Bassel, Phys. Rev. **155**, 1194 (1967).
- <sup>18</sup>J. C. Hafele, E. R. Flynn, and A. G. Blair, Phys. Rev. **155**, 1238 (1967).
- <sup>19</sup>R. A. Hinrichs, R. Sherr, G. M. Crawley, and I. Proc-tor, Phys. Rev. Lett. **25**, 829 (1970).
- <sup>20</sup>W. R. Coker, T. Udagawa, and H. H. Wolter, Phys. Lett. **41B**, 237 (1972); Phys. Rev. C **7**, 1154 (1973); Phys. Lett. **46B**, 27 (1973); N. B. De Takacsy, *ibid.* **42B**, 1 (1972); M. Toyama, Nucl. Phys. **A211**, 254 (1973).
- <sup>21</sup>A. E. L. Dieperink, and P. W. M. Glaudemans, Phys. Lett. **28B**, 531 (1969).
- <sup>22</sup>B. H. Wildenthal, E. C. Halbert, J. B. McGrory, and T. T. S. Kuo, Phys. Rev. C **4**, 1267 (1971) (wave functions closely similar to those in Ref. 21).
- <sup>23</sup>L. D. Skouras, Phys. Lett. **31B**, 439 (1970), and private communication.
- <sup>24</sup>A. Richter, J. R. Comfort, V. Anantaraman, and J. P. Schiffer, Phys. Rev. C **5**, 821 (1972).
- <sup>25</sup>G. C. Ball and J. Cerny, Phys. Rev. **177**, 1466 (1969).
- <sup>26</sup>R. Schaeffer, unpublished calculations based on the data in Ref. 25.
- <sup>27</sup>L. D. Skouras, private communication.
- <sup>28</sup>R. Schaeffer, J. Raynal, program DWBA74, CEN Saclay (unpublished).
- <sup>29</sup>L. D. Rickertsen, M. J. Schneider, J. J. Kraushaar, W. R. Zimmerman, and H. Rudolph, Phys. Lett. **60B**, 19 (1975).
- <sup>30</sup>L. D. Rickertsen and P. D. Kunz, Phys. Lett. **47B**, 11 (1973).
- <sup>31</sup>D. C. Weisser, J. S. Lilley, R. K. Hobbie, and G. W. Greenlees, Phys. Rev. C **2**, 544 (1970).
- <sup>32</sup>L. A. Charlton and P. D. Kunz, Phys. Lett. **72B**, 7 (1977).
- <sup>33</sup>F. Osterfeld, T. Udagawa, and H. H. Wolter, Nucl. Phys. **A278**, 1 (1977).
- <sup>34</sup>See AIP Document No PAPS PRVCA-19-19-27 for 27 pages of  $^{38}\text{Ar}(^3\text{He}, t)^{38}\text{K}$  experimental angular distributions. Order by PAPS number and journal reference from American Institute of Physics, Physics Auxiliary Publication Service, 335 East 45th Street, New York, NY 10017. The price is \$1.50 for microfiche, or \$5 for photocopies, Airmail additional. Make checks payable to the American Institute of Physics. This material also appears in *Current Physics Microform*, the monthly microfilm edition of the complete set of journals published by AIP, on the frames immediately following this journal article.